This is an extended version of the paper presented in SEE7 conference, peer-reviewed again and approved by the JSEE editorial board.

An Analytical Model for Steel Shear Wall Strengthened with CFRP Using Composite Theory

Technical Note

Majid Gholhaki[1*] and Younes Nouri[2]

1. Assistant Professor, Semnan University, Semnan, Iran, * Corresponding Author; email: mgholhaki@semnan.ac.ir
2. B.Sc. Student, Semnan University, Semnan, Iran

Received: 01/11/2015
Accepted: 16/12/2015

ABSTRACT

In this paper, steel plate shear wall strengthened by Carbon Polymer's Fiber was studied. An equation has been proposed for elastic strength using composite theory and maximum work failure model, and another equation has been obtained for elastic displacement related to polymer's fiber using virtual work principle. Considering fibers and shear wall web as a layer and super positioning plate and fiber behavior, composite shear wall model was achieved. Optimum fiber orientation angle for composite shear wall was in diagonal tension field. Finite element values via the presented model were compared and concluded that the offered model can predict composite shear wall in close range. The proposed model can predict the elastic strength and displacement of composite steel plate shear wall that strengthened with CFRP layers. In this model, the over strength due to CFRP layers super positioned to PFI model and the overall response of composite shear wall can be achieved.

Keywords:
Composite steel shear wall; CFRP; Diagonal tension field; Virtual work; Elastic strength

1. Introduction

Steel shear wall can significantly tackle and tolerate lateral loads due to the wind and earthquake through diagonal tension field of steel plates confined between boundary elements of system [1]. The first philosophy of steel shear wall design was based on preventing global buckling in plate; however, it was later seen that most of the post shear strength of shear wall was achieved after buckling of plate [2-3]. These shear walls were initially utilized as a retrofit system; however, after their good performance was approved, they were applied as a structure system. Some advantages of this system are high ductility, energy absorption, stiffness and strength, on the contrary, the disadvantage of this system is low elastic strength of steel walls. To improve shear performance of steel shear walls, adding vertical and horizontal stiffeners [3], low yield point plate materials [4], strengthening with concrete [5-7], perforated web plate [5], and covering steel plate with FRP materials [8-10] have been studied. Due to light weight, high elasticity module and high tension strength, FRP materials have a wide application in civil engineering. Covering plate with FRP increases the shear strength, energy absorption, excessive post buckling field distribution and stiffness of shear wall. So far, the configuration of fiber orientation, behavior and seismically parameters of composite steel shear wall have been evaluated by numerical and empirical methods [9], and yet, no explicit analytical method has been presented, but the experimental and numerical studies absolutely depend on the dimension

Table 1. Mechanical properties of steel materials.

	Elastic Modules	Yield Stress	Yield Strain	Ultimate Stress	Ultimate Strain	Rupture Strain
	GPA	MPA	%	MPA	%	%
Plate	204	197	0.097	323.2	25	26
UNP 100	203	310	0.23	460.5	18	19

and mechanical properties of steel and FRP. Two major analytical methods have been presented for the analysis of steel shear wall that are stripe model [11] and plate-frame interaction [12]. Plate - frame interaction in most cases yields the precise values. In Hatami et al. [8], some specimen strengthened with CFRP layers have been studied, and in these experimental tests, fiber orientations, thickness of CFRP and shear wall dimension under cyclic loading were evaluated. Finally, some equations were proposed for nonlinear behavior of CSSW using elastic analysis. In Rahai and Alipour [10] evaluated the ductility, stiffness, yield shear force factors under push over analysis as well as the thickness of FRP layers. They concluded that in diagonal tension field, overall strength and stiffness of shear wall have been increased. In addition, Nateghi-Alahi and Khazaei-Poul [9] conducted five experimental tests on composite steel shear wall under cyclic loading, different fiber angle and thickness. They concluded that the fiber inclination is the most important variable on behavior of composite shear wall; moreover, they concluded that the initial and secant stiffness of CSSW would increase if principal orientation of fiber material is in tension field angle. In this article, over-strength and seismic parameter of composite steel plate shear wall, strengthened with FRP materials using analytical and almost simple methods, have been studied. Furthermore, stress and strain in FRP material in different fiber angles, extra strength due to FRP, stiffness of shear wall after adding FRP and elastic shear displacement in FRP were achieved using these equations.

2. Verification

According to Nateghi-Alahi and Khazaei-Poul [9], to calibrate FEM software, an experimental test was selected and simulated with FEM software. In experimental test, CSPSP3 was chosen because it is strengthened with one layer FRP on each side at fiber orientation 45/-45 degree. This specimen is more consistent with FEM simulation of this study. The dimension of CSPSP3 is shown in Figure (1). Material properties of infill plate and boundary element of SPSW are tabulated in Table (1). In addition, FRP Characteristics are listed in Table (2).

The numerical push-over curve for both FEM and Experimental tests are presented and compared in Figure (2). It is concluded that FEM simulation

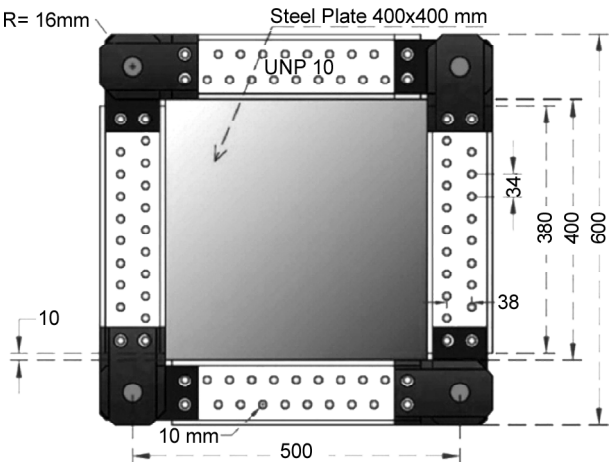

Figure 1. Experimental scheme based on Nateghi-Alahi.

Table 2. Mechanical properties of FRP.

Tensile Modulus		Tensile Strength	
Ex (GPA)	Ey (GPA)	Tx (MPA)	Ty (MPA)
26.49	7.07	537	23

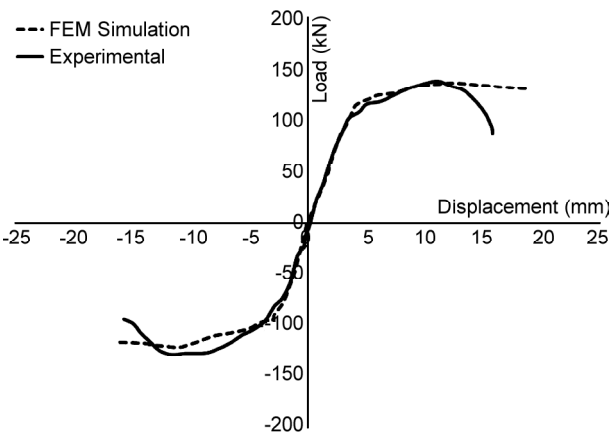

Figure 2. Good agreement of experimental and FEM simulations.

has been successful in estimating the shear capacity and behavior of CSPSP3.

3. Composite Structural Analysis

The analysis of composite structures is more complicated than that of conventional metallic structures. While metallic structures can usually be treated as isotropic materials, in which the properties do not depend on orientation, composite materials are not homogeneous and are anisotropic in nature. Consider the single ply shown in Figure (3), two right-hand coordinate systems is shown.

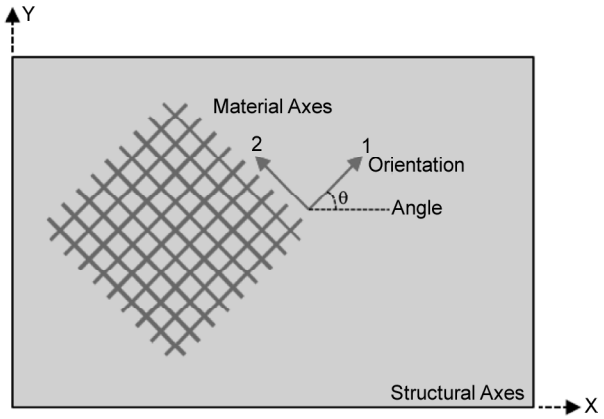

Figure 3. Structural and material axes.

The 1-2 system is known as the principal material axes system, with the 1-direction parallel or longitudinal to the fiber direction (zero-degree) and the 1-direction perpendicular or transverse to the fiber direction (90-degree). The second system, represented by x-y, is the structural loading direction or the direction in which loads are applied to the ply. The angle θ between the x-axis and the 1-axis is called the fiber orientation angle. The stresses in the structural axes (σ_{xx},σ_{yy} and σ_{xy}) can be obtained from those in the material axes (σ_{11}, σ_{22}, and τ_{11}) by Eq. (1) [13-14].

$$\begin{bmatrix}\sigma_{xx}\\ \sigma_{yy}\\ \tau_{xy}\end{bmatrix}=\begin{bmatrix}m^2 & n^2 & -2mn\\ n^2 & m^2 & 2mn\\ mn & -mn & m^2-n^2\end{bmatrix}\begin{bmatrix}\sigma_{11}\\ \sigma_{22}\\ \tau_{12}\end{bmatrix} \quad (1)$$

where $m=\cos\theta$ and $n=\sin\theta$. Figure (4) presents the stress in structural axes and material axes. Similarly, the strain in material axes can be transformed to structural axes by Eq. (2).

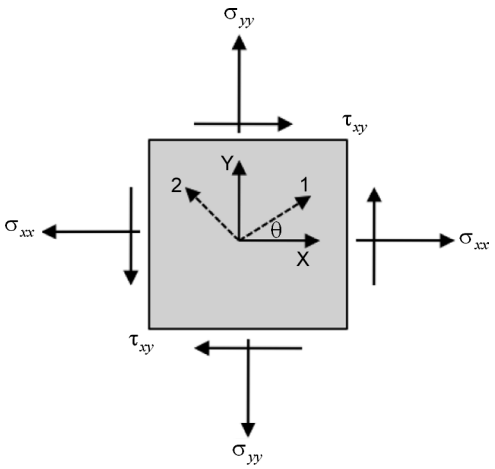

Figure 4. Stress in structural and materials axes.

$$\begin{bmatrix}\varepsilon_{xx}\\ \varepsilon_{yy}\\ \gamma_{xy}\end{bmatrix}=\begin{bmatrix}m^2 & n^2 & -mn\\ n^2 & m^2 & mn\\ 2mn & -2mn & m^2-n^2\end{bmatrix}\begin{bmatrix}\varepsilon_{11}\\ \varepsilon_{22}\\ \gamma_{12}\end{bmatrix} \quad (2)$$

The Stress-Strain relationship for a single ply, loaded by off-axis to the material was obtained from Eq. (3).

$$\begin{bmatrix}\sigma_{xx}\\ \sigma_{yy}\\ \tau_{xy}\end{bmatrix}=\begin{bmatrix}\overline{Q}_{11} & \overline{Q}_{12} & \overline{Q}_{16}\\ \overline{Q}_{21} & \overline{Q}_{22} & \overline{Q}_{26}\\ \overline{Q}_{16} & \overline{Q}_{26} & \overline{Q}_{66}\end{bmatrix}\begin{bmatrix}\varepsilon_{xx}\\ \varepsilon_{yy}\\ \gamma_{xy}\end{bmatrix} \quad (3)$$

where $[\overline{Q}]$ is the stiffness matrix and $[Q]$ is the stiffness coefficient. The elements of $[\overline{Q}]$ are defined as follows:

$$\overline{Q}_{11}=U_1+U_2\cos 2q+U_3\cos 4q \quad (4)$$

$$\overline{Q}_{12}=\overline{Q}_{21}=U_4-U_3\cos 4q \quad (5)$$

$$\overline{Q}_{16}=1/2U_2\sin 2q+U_3\sin 4q \quad (6)$$

$$\overline{Q}_{22}=U_1-U_2\cos 2q+U_3\cos 4q \quad (7)$$

$$\overline{Q}_{26}=1/2U_2\sin 2q-U_3\sin 4q \quad (8)$$

$$\overline{Q}_{66}=U_5-U_3\cos 4q \quad (9)$$

where U_1 through U_5 were obtained from Eqs. (10) to (14).

$$U_1=1/8\left(3Q_{11}+3Q_{22}+2Q_{12}+4Q_{66}\right) \quad (10)$$

$$U_2=1/2\left(Q_{11}-Q_{22}\right) \quad (11)$$

$$U_3=1/8\left(Q_{11}+Q_{22}+2Q_{12}-4Q_{66}\right) \quad (12)$$

$$U_4=1/8\left(3Q_{11}+3Q_{22}+6Q_{12}-4Q_{66}\right) \quad (13)$$

$$U_5 = 1/2\left(U_1 - U_4\right) \tag{14}$$

Also, elements of [Q] matrix were defined as Eqs. (15) to (18).

$$Q_{11} = \frac{E_1}{1 - J_{12}J_{21}} \tag{15}$$

$$Q_{12} = \frac{J_{21}E_1}{1 - J_{12}J_{21}} \tag{16}$$

$$Q_{22} = \frac{E_2}{1 - J_{12}J_{21}} \tag{17}$$

$$Q_{66} = G_{12} \tag{18}$$

The relationship between major Poisson's ratio and minor Poisson's ratio is expressed as Eq. (19).

$$\frac{J_{12}}{E_{11}} = \frac{J_{21}}{E_{22}} \tag{19}$$

The elastic constants for an angle ply or off-axis ply can be calculated using Eqs. (20) to (24).

$$E_{yy} = \left[\frac{n^4}{E_{11}} + \frac{1}{G_{12}} - \frac{2J_{12}}{E_{11}}m^2n^2 + \frac{m^4}{E_{22}}\right]^{-1} \tag{20}$$

$$E_{xx} = \left[\frac{m^4}{E_{11}} + \frac{1}{G_{12}} - \frac{2J_{12}}{E_{11}}m^2n^2 + \frac{n^4}{E_{22}}\right]^{-1} \tag{21}$$

$$G_{xy} = \left[\frac{4}{E_{11}} + \frac{4}{E_{22}} + \frac{8J_{12}}{E_{11}} - \frac{2}{G_{12}}\frac{m^2n^2}{E_{11}} + \left(\frac{m^4 + n^4}{G_{12}}\right)\right]^{-1} \tag{22}$$

$$J_{xy} = E_{xx}\left[\frac{J_{12}(m^4 + n^4)}{E_{11}} - \frac{1}{E_{11}} + \frac{1}{E_{22}} - \frac{1}{G_{12}}m^2n^2\right] \tag{23}$$

$$J_{yx} = J_{xy}\frac{E_{yy}}{E_{xx}} \tag{24}$$

3.1. Failure Theories

Failure prediction for metallic structures is normally performed by comparing stresses or strains caused by applied loads with the allowable strength or strain capacity of the material. For isotropic materials that exhibit yielding, either the Tresca maximum shear stress theory or von Mises distortional energy theory is commonly used. However, composites are not isotropic and do not yield. Failure modes in composites are generally noncatastrophic and may involve localized damage via such mechanisms as fiber breakage, matrix cracking, debonding, and fiber pull-out. These can progress simultaneously and interactively, making failure prediction for composite complexes. There are five independent strength constants that are important for a single ply.

- S_{Lt} or ε_{Lt} - longitudinal tensile strength or strain
- S_{Tt} or ε_{Tt} - transverse tensile strength or strain
- S_{Lc} or ε_{Lc} - longitudinal compressive strength or strain
- S_{Tc} or ε_{Tc} - transverse compressive strength or strain
- S_S or γ_S - in-plane shear strength or strain.

3.1.1. Maximum Stress Criterion

According to this theory, failure occurs when any stress in the principal material directions is equal to or greater than the corresponding allowable strength.

3.1.2. Maximum Strain Theory

The maximum strain theory is very similar to the maximum stress theory except that strains are used instead of stresses. According to this theory, failure will occur if any strain in the principal material axes is equal to or greater than the corresponding allowable strain.

3.1.3. Azai-Tsai-Hill Maximum Work Theory

The maximum work theory states that for plane stress, failure initiates when the inequality Eq. (25) is violated.

$$\frac{s_{11}^2}{S_{Lt}^2} - \frac{s_{11}s_{22}}{S_{Lt}^2} + \frac{s_{22}^2}{S_{Tt}^2} + \frac{t_{12}^2}{S_S^2} < 1 \tag{25}$$

The advantage of the Azai-Tsai-Hill criterion is that the interaction between strengths and failure modes is taken into account. Figure (5) shows the difference between these criteria.

4. SPSW - FRP Composite Model

4.1. Optimum Fiber Orientation Angle

Based on FE models and reports on Nateghi-Alahi and Khazaei-Poul [9], if principal orientation of FRP layers is oriented in the direction of diagonal tension field, the shear strength and stiffness of

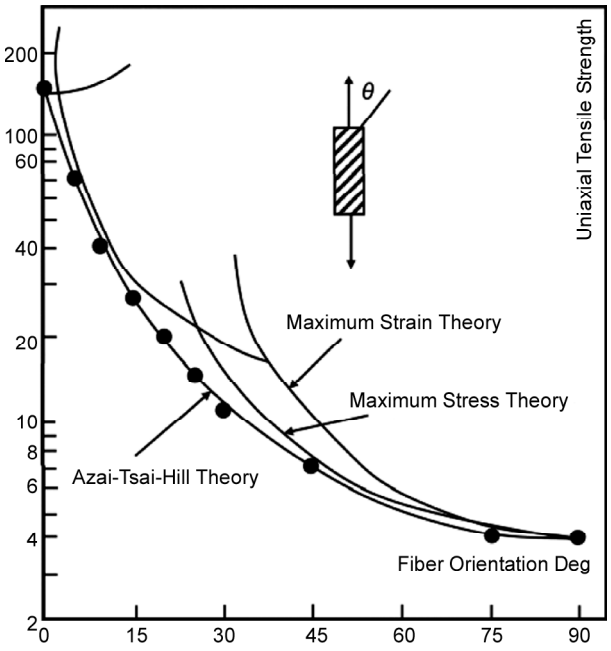

Figure 5. Failure criterion.

composite shear wall will increase. Because tensile strength in principal direction of FRP is greater than transverse tensile strength, then placing main fiber direction in diagonal tension of plate increases shear strength and stiffness of composite shear wall.

4.2. FRP Elastic Shear Strength

Using Eq. (1) and assuming that S_{xx} and S_{yy} are negligible in fiber element, the stresses in fiber element written as Eqs. (26) to (28).

$$\sigma_{11} = 2mnt_{xy} \tag{26}$$

$$\sigma_{22} = -2mnt_{xy} \tag{27}$$

$$\tau_{12} = (m^2 - n^2)t_{xy} \tag{28}$$

Substitution of Eqs. (27), (28), and 29 into (26) yields Eq. (30).

$$t_{xy} = \left[\frac{8m^2n^2}{S_{Lt}^2} + \frac{4m^2n^2}{S_{Tt}^2} + \frac{(m^2-n^2)^2}{S_s^2}\right]^{-\frac{1}{2}} \tag{29}$$

The over shear strength in CSPSW, due to FRP, was achieved by integration of Eq. (29) over the FRP area that yields Eq. (30).

$$U_{frp} = \left[\frac{8m^2n^2}{S_{Lt}^2} + \frac{4m^2n^2}{S_{Tt}^2} + \frac{(m^2-n^2)^2}{S_s^2}\right]^{-\frac{1}{2}} bt \tag{30}$$

4.3. FRP Elastic Shear Displacement

To evaluate FRP in CSPSW, elastic displacement must be determined. For this reason, the internal strain energy in material and the work done by external shear force must be equal. Strain energy density function is stated as Eq. (31).

$$U_0 = \frac{m^4 s_{11}^2}{2E_{xx}} + \frac{n^4 s_{11}^2}{2E_{yy}} + \frac{m^2n^2 s_{11}^2}{2G_{xy}} \tag{31}$$

Strain energy in FRP layer written as Eq. (32).

$$U_{strain\ energy} = \iiint U_0 dV \tag{32}$$

After integrating Eq. (32) over the volume in which the energy is stored, the strain energy is obtained, Eq. (33).

$$U_{SE} = \left(\frac{m^4 s_{11}^2}{2E_{xx}} + \frac{n^4 s_{11}^2}{2E_{yy}} + \frac{m^2n^2 s_{11}^2}{2G_{xy}}\right) bdt \tag{33}$$

The work done by external shear force is stated as Eq. (34).

$$W_{shear\ force} = 1/2 F_{frp} U_{frp} \tag{34}$$

Putting Eq. (33) and Eq. (34) equal, gives the elastic shear displacement, Eq. (35).

$$U_{frp} = \left(\frac{m^4}{E_{xx}} + \frac{n^4}{E_{yy}} + \frac{m^2n^2}{G_{xy}}\right) \frac{s_{11}^2 bdt}{F_{frp}} \tag{35}$$

Substituting Eq. (30) in Eq. (35) yields the Elastic shear displacement, Eq. (36).

$$U_{frp} = \left(\frac{m^4}{E_{xx}} + \frac{n^4}{E_{yy}} + \frac{m^2n^2}{G_{xy}}\right) \times \left(\frac{8m^2n^2}{S_{Lt}^2} + \frac{4m^2n^2}{S_{Tt}^2} + \frac{(m^2-n^2)}{S_s^2}\right)^{\frac{1}{2}} s_{11}^2 d \tag{36}$$

In elastic state, $s_{11} = S_{Lt}$.

5. Results and Discussion

Three specimens that have one story steel plate shear wall have been considered to evaluate the effects of FRP on maximum strength and behavior of composite SPSW. The dimensions and boundary element of these specimens are shown in Table (3). The connections in frame are rigid. SPSW strengthened is with two layers of FRP,

Table 3. CSSW dimensions and sections.

	b (m)	d (m)	t (mm)	Beam	Column
CSSW1	3.2	1.7	4	W10x39	W10x39
CSSW2	3.3	2.3	5	W10x45	W10x45
CSSW3	2	2.9	5	W10x49	W10x49

one layer in each side. Thickness of each layer is 0.5 mm.

FRP materials are tabulated in Table (4). The materials considered for frame and plate are conventional steel with $f_y = 240$ MPA and $f_u = 370$ MPA. Fiber orientation angle is measured in respect to horizontal and increases from 0 - 90 degrees to investigate over strength due to FRP layers. Figure (6) shows the fiber angle.

Force - displacement diagram for specimens are shown in Figures (7), (8) and (9). In each push curve, maximum over strength of FRP has been considered. Optimum fiber angle as mentioned earlier is in diagonal tension field and only the highest curve of push over analysis is shown in Figures (7) to (9).

Table 4. FRP mechanical properties.

	E11 (GPA)	E22 (GPA)	G12 (GPA)	ν12
	140	10	5	0.28
S_{Lt} (MPA)	S_{Tt} (MPA)	S_{Tc} (MPA)	S_s (MPA)	S_{Lc} (MPA)
1500	50	250	70	1200

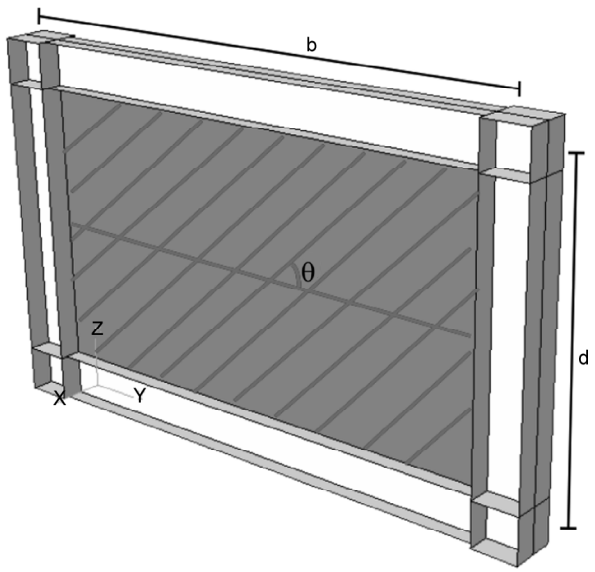

Figure 6. Fiber orientation angle.

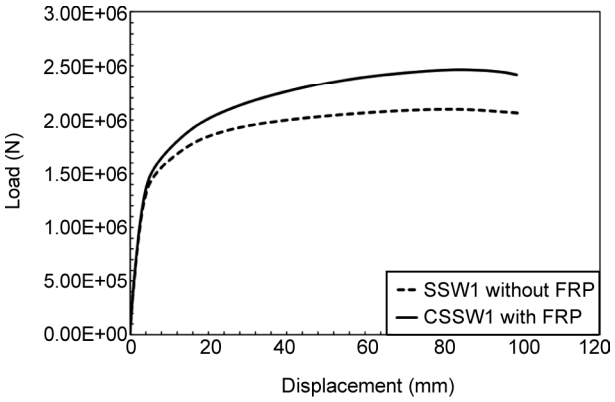

Figure 7. Shear force - displacement diagrams for CSSW1 and SSW1.

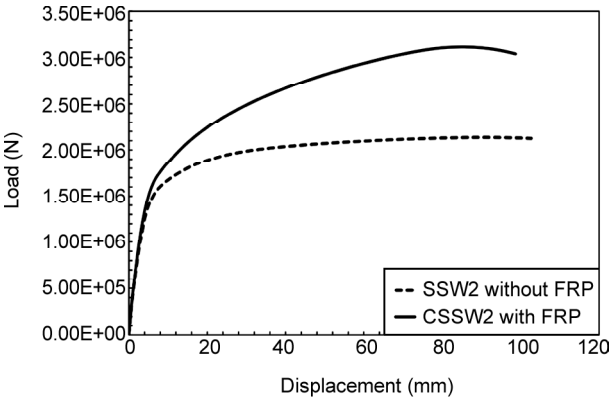

Figure 8. Shear force - displacement diagrams for CSSW2 and SSW2.

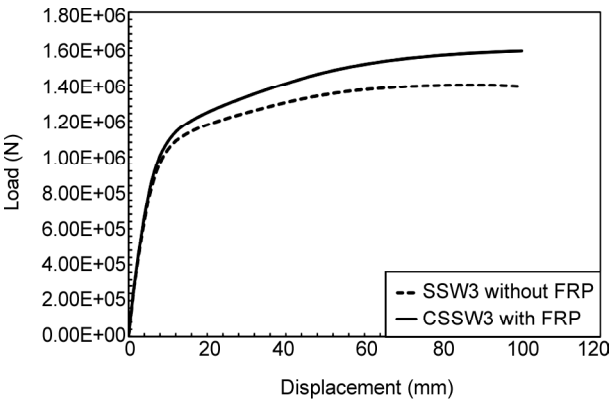

Figure 9. Shear force - displacement diagrams for CSSW3 and SSW3.

Tension field angle is based on Thorburn et al. [11] and is formulated as Eq. (37). Although α is measured in respect to the vertical axis, since in this article, the base angle is measured in respect to the horizontal axis, tension field angle is $\theta = \pi/2 - \alpha$.

$$\tan^4 \alpha = \left(1 + \frac{t_w L}{2A_c}\right) \Big/ \left(1 + t_w h\left[\frac{1}{A_b} + \frac{h^3}{360 I_c L}\right]\right) \qquad (37)$$

Tension field angle has been calculated for each specimen and is shown in Table (5).

Table 5. Tension field angle.

	CSSW1	CSSW2	CSSW3
θ (deg)	35.59	40.89	50.63

To evaluate the steel shear wall without FRP, PFI method has been considered [12]. In Figure (10), the elastic strength and elastic displacement of plate, frame and shear wall are shown. Eqs. (38) to (42) describes coordinates of parametric push over curve.

$$F_{wu} = \left(t_{cr} + 1/2\, s_{ty} \sin(2q)\right) bt \tag{38}$$

$$t_{cr} = \frac{Kp^2 E}{12(1-m^2)} \left(\frac{t}{b}\right)^2 \tag{39}$$

$$U_{we} = \frac{2 s_{ty} d}{E \sin(2q)} \tag{40}$$

$$F_{fe} = 4 M_{fp} / d \tag{41}$$

$$U_{fe} = \frac{M_{fp} d^2}{6 E I_f} \tag{42}$$

Using PFI method [12] and Eq. (30) and Eq. (36), parametric push curve for steel plate without FRP, strengthened with FRP, is achieved and has been compared to FEM curves. The superposition push-over curve for the composite steel plate shear wall is shown in Figure (11). In PFI method, the tension field angle considered as optimum fiber angle of FRP material. Calculations of PFI parameter are summarized in Table (6). Also, the critical shear buckling stress has been neglected.

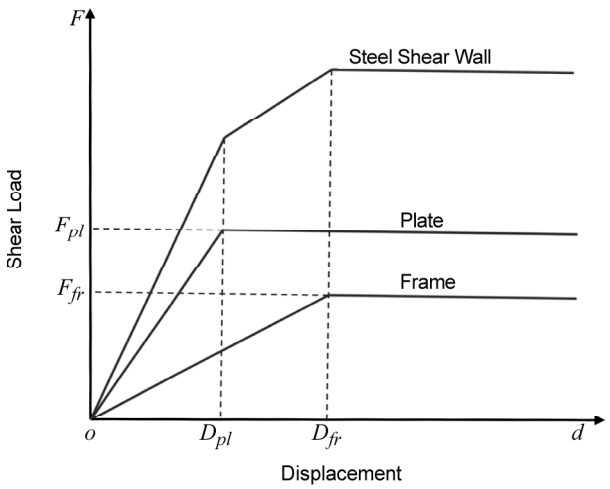

Figure 10. Parametric load-displacement curve based on PFI.

Table 6. Parameters of PFI Push-over curve.

	F_{pl} (KN)	D_{pl} (mm)	F_{fr} (KN)	D_{fr} (mm)
SSW1	1847.1	4.22	379.2	4.62
SSW2	1933.9	5.41	329.6	8.2
SSW3	1176.9	6.76	295.1	12.61

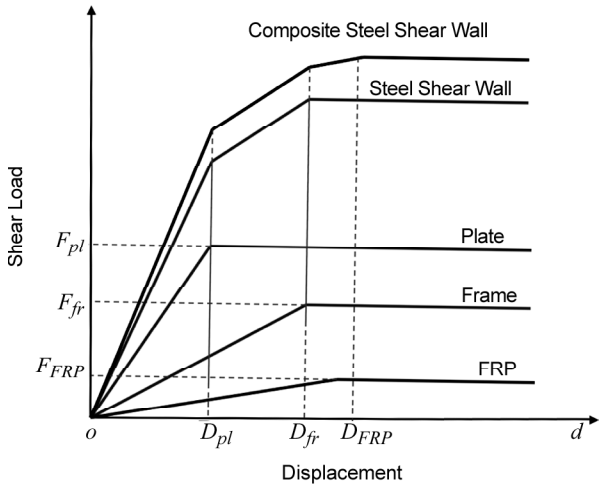

Figure 11. Parametric load-displacement curve for composite shear wall.

Over strength due to FRP on SSW has been calculated for three specimens and superposition with PFI curves, because Eq. (30) and Eq. (37) achieved in elastic region superposition are valid. Overall force-displacement of composite shear wall for each specimen is shown in Figures (12) to (14) and these curves are compared with FEM push-over curves.

As shown in Figures (12) to (14), the theoretical

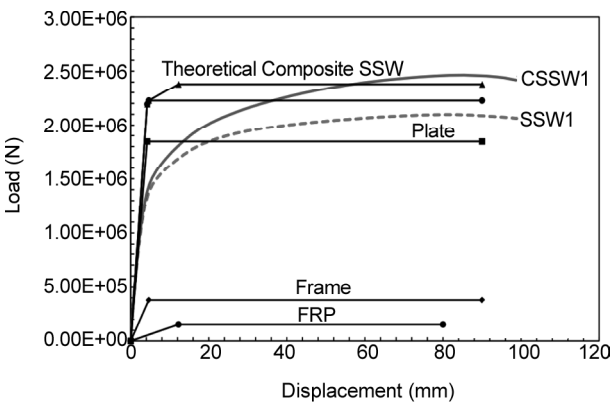

Figure 12. Theoretical curve for composite SSW1 and FEM simulation.

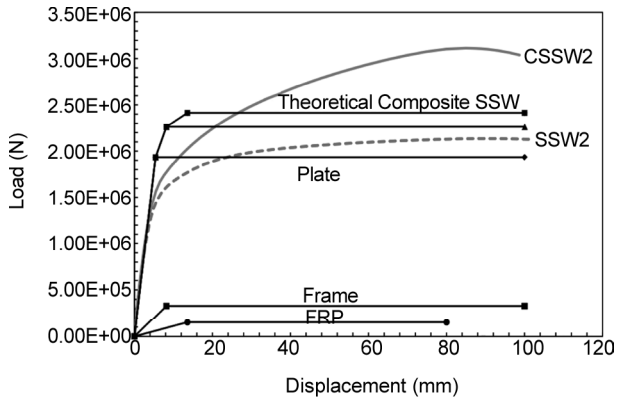

Figure 13. Theoretical curve for composite SSW2 and FEM simulation.

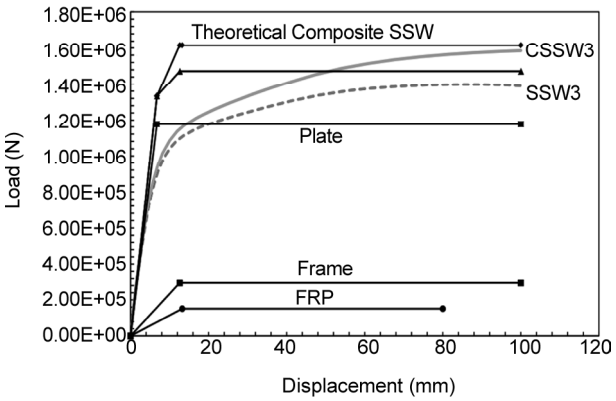

Figure 14. Theoretical curve for composite SSW3 and FEM simulation.

Eq. (30) and Eq. (36) for predicting FRP elastic displacement and over shear strength are completely consistent with FE models.

6. Conclusion

- Using composite structural analysis, some equations are obtained for elastic shear strength and elastic shear displacement for composite steel shear walls.
- Azai-Tsai-Hill yields the most reliable result in estimation overall response of composite steel plate shear wall.
- For shear strength and maximum stress criterion yields the most reliable estimate for elastic shear displacement.
- Using stress - strain Eqs. (3) to (19) given in this article, stress and strain can be obtained in arbitrary direction in FRP material.

References

1. Astaneh-Asl, A. (2002) *Seismic Behavior and Design of Composite Steel Plate Shear Walls, Steel Tips*. Structural Steel Educational Council, Technical Information & Product Service.
2. Wagner, H. (1931) *Flat Sheet Metal Girders with Very Thin Webs*. Tech No. 604, National Advisory Committee for Aerodynamics, Washington, D.C.
3. Takahashi, Y., Takemoto, Y., Takeda, T., and Takagi, M. (1973) *Experimental Study on Thin Steel Shear Walls and Particular Bracing under Alternative Horizontal Load*. Preliminary Report, Lisbon, Portugal, 185-191.
4. Kharrazi, M.H.K. (2005) *Rational Methods for Analysis and Design of Steel Plate Shear Walls*. Ph.D. Dissertation, University of British Colombia.
5. Vian, D., Bruneau, M. (2004) Testing of special LYS steel plate shear walls. *13th World Conf. on Earthquake Engineering*, Report No. 978, Canada.
6. Rahai, A. and Hatami, F. (2009) Evaluation of composite shear wall behavior under cyclic loadings. *Journal of Constructional Steel Research*, **65**, 1528-1537.
7. Arabzadeh, A., Soltani, M., and Ayazi, A. (2011) Experimental investigation of composite shear walls under shear loadings. *Thin-Walled Structures*, **49**, 842-854.
8. Hatami, F., Ghamari, A., and Rahai, A. (2012) Investigating the properties of steel shear walls reinforced with Carbon Fiber Polymers (CFRP). *Journal of Constructional Steel Research*, **70**, 36-42.
9. Nateghi-Alahi, F. and Khazaei-Poul, M. (2012) Experimental study of steel plate shear walls with infill plates strengthened by GFRP laminates. *Journal of Constructional Steel Research*, **78**, 159-172.
10. Rahai, A. and Alipour, M. (2011) Behavior and Characteristics of Innovative Composite plate Shear Walls. *Procedia Engineering*, **14**, 3205-3212.
11. Thorburn L.J., Kulak G.L., and Montgomery C.J.

(1983) *Analysis of Steel Plate Shear Walls*. Structural Engineering Report No. 107.

12. Roberts, T.M. and Sabouri-Ghomi, S. (1991) Hysteretic characteristics of unstiffened plate shear panels. *Thin-Walled Structures*, **12**, 145-162.

13. Valery (2001)

14. Jones, R.M. (1999) *Mechanics of Composite Materials*. Taylor & Francis, Inc., USA.

?. Vasiliev, V.V. and Morozov, E. (2001) *Mechanics and Analysis of Composite Materials*. 1st Edition, Elsevier Science Publication, Netherlands.